SPECIAL ISSUE - RESEARCH ARTICLE

WILEY *Journal of* RAMAN SPECTROSCOPY

New insights into the degradation mechanism of cellulose nitrate in cinematographic films by Raman microscopy

Artur Neves [ID] | Eva Mariasole Angelin [ID] | Élia Roldão [ID] | Maria João Melo [ID]

Department of Conservation and Restoration and LAQV-REQUIMTE, Faculty of Sciences and Technology, NOVA University of Lisbon, Campus da Caparica, 2829-516 Caparica, Portugal

Correspondence
Maria João Melo, Department of Conservation and Restoration and LAQV-REQUIMTE, Faculty of Sciences and Technology, NOVA University of Lisbon, Campus da Caparica, Caparica 2829-516, Portugal.
Email: mjm@fct.unl.pt

Abstract

The degradation of cellulose nitrate cinematographic films stored inside an aluminum can was studied by infrared spectroscopy and Raman microscopy. Cellulose nitrate image heritage is strongly susceptible to degradation, being a major conservation challenge. Infrared spectroscopy has been the traditional technique in the assessment of the polymer degradation, but new in situ diagnostic tools to monitor the initial stages of degradation are needed. In this work, cellulose nitrate films were produced and irradiated as aging references to understand how chemical changes were observed in Raman spectroscopy. In comparison with infrared spectroscopy, this technique confirmed the mechanisms proposed in the literature and, at advanced stages of degradation, provided new relevant information detecting an intense peak at 1046 cm^{-1} associated to nitric acid. Comparing these results with the cinematographic films, it was observed that the plasticizers, which identification was more straightforward using Raman microscopy, have contributions in the regions were chemical changes occur, making it difficult to draw conclusions. Nevertheless, nitric acid and silver nitrate peaks were found in Raman spectra confirming the unstable and noxious environment inside de aluminum can and proving that Raman microscopy can be a valuable complementary in situ technique for cellulose nitrate degradation studies.

KEYWORDS
celluloid, cellulose nitrate, cinematographic films, degradation mechanisms, photooxidation

1 | INTRODUCTION

Cellulose nitrate is considered the first semi synthetic polymer and the advent of plastic industry.[1–3] It was obtained substituting hydroxyl by nitrate groups in cellulose-based materials (e.g., paper and cotton), and for a nitrogen content higher than 12%, cellulose nitrate was an explosive material used for military ends.[3] Lowering the degree of nitration and adding camphor as a plasticizer, a workable plasticized material could be produced, overcoming the embrittlement problem of pure cellulose nitrate. This discovery paved the way to a wide range of applications, such as commodities, films, and paints. There is still dispute concerning who first has discovered the importance of camphor in this new formulation, but there are no doubts that Alexander Parkes (UK) and John Wesley Hyatt (USA) made original outstanding contributions and trademarked their discoveries as Parkesine™ (1862) and Celluloid™ (1872).[2,3] The flexibility and dimensional stability of cellulose nitrate led to its extensive use as a new photographic and cinematographic medium for films. Later, camphor began to be replaced by other plasticizers, namely, phthalates after the 1920s and triphenyl and tricresyl phosphates after

World War II.[4] Widely used between 1890s and 1950s, it is the main component of image heritage in archives and museums. Due to its flammability, the production of cellulose nitrate films ceased in 1951 for safety reasons.[5]

Cellulose nitrate is an unstable material that poses threats to museum and archival collections. This polymer degrades at a very high rate leading to yellowing, embrittlement, and cracking which, in turn, can lead to the material collapse. It is also hazardous by releasing nitric acid, a highly oxidizing and corrosive acid.[4,6,7] Two preservation options are presently applied: "cool" or "cold" storage.[8] These options present high costs, and their effects on the mechanical and chemical behavior of the polymer still demand further work. In addition, they do not solve or prevent the problem because the reaction continues to occur, only at a slower rate, and for objects which are meant to be displayed, these are not practical solutions.

A full understanding of the complex degradation mechanisms that cause the collapse of the cellulose nitrate matrix, coupled with in situ early warning systems, will provide the ground for the development of sustainable conservation treatments that are crucially needed. Raman spectroscopy has already been successful applied in the characterization of nitrocellulose-based materials in cultural heritage.[9,10] In this work, it was used to get insight into the photodegradation mechanism of cellulose nitrate and the main intermediates formed in artificially aged films and in naturally aged cinematographic films. For example, we aim at testing its potential in the molecular characterization of hydroperoxides, a fundamental intermediate in the first degradation stages, as the O—O stretching vibration band should have strong intensity in Raman between 900 and 800 cm^{-1}.[11] The results obtained will be compared with infrared spectroscopy. To the best of our knowledge, Raman spectroscopy was used for the first time in the study of cellulose nitrate photodegradation.

2 | CELLULOSE NITRATE DEGRADATION MECHANISMS

Thérias et al.[12] proved that photooxidation simulates the natural cellulose nitrate degradation mechanism. According to the literature, the initial stage of cellulose nitrate degradation is characterized by the homolytic scission of the NO bond in nitrate groups, in the most labile C2 or C3 positions, with the release of $^\bullet NO_2$.[12–16] This radical can be subsequently transformed, by $^\bullet$H abstraction or reaction with water, into the pair nitrous acid/nitric acid (HNO_2/HNO_3), according to the reactions depicted in Figure 1a.[17,18] In the end, a complete loss of the nitrate substitution in the cellulose ring will be observed.

If $^\bullet$H abstraction occurs at C1, hydroperoxides formation and further decomposition will promote a continuous chain scission process through the formation of carbonyl intermediates, namely, gluconolactones and anhydrides, with release of methyl nitrate (CH_3ONO_2), Figure 1b. The photooxidation of the degradation products formed leads to the total loss of the polymer through the emission of high quantity of volatiles with low molecular weight.

It is important to note that HNO_2 and HNO_3 are the most hazardous degradation products in the preservation
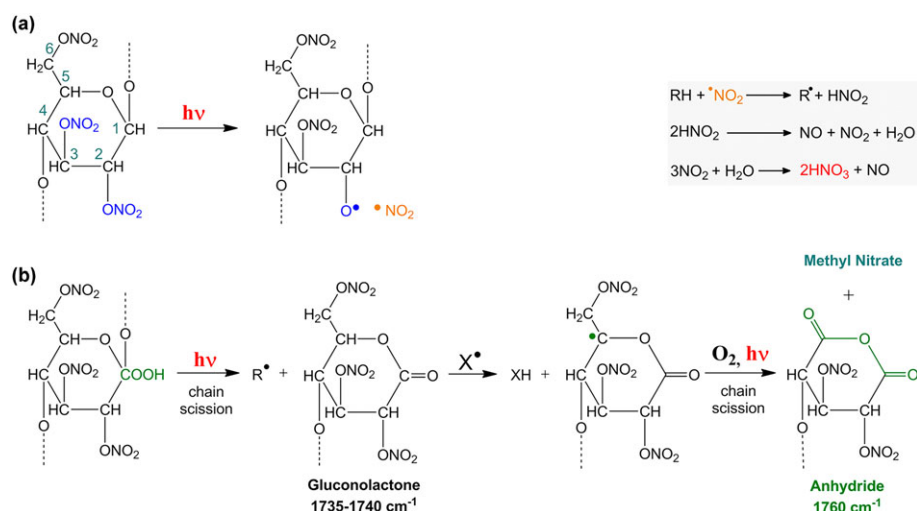

FIGURE 1 (a) First phase of cellulose nitrate degradation mechanism, which starts with the homolytic scission of a nitrate group in C2 or C3 positions and release of $^\bullet NO_2$. These radicals lead to H$^\bullet$ abstractions and formation of HNO_2 and HNO_3 according to the described reactions. (b) The excited state hydroperoxide leads to glycosidic bond cleavage with formation of a gluconolactone. This intermediate is then transformed into an anhydride with release of $^\bullet CH_2ONO_2$, which converts into a final product, methyl nitrate, by $^\bullet$H abstraction

of cellulose nitrate collections and archives. In addition to being highly oxidizing, the pH decrease also induces hydrolysis reactions, which can lead to further chain breakdown and formation of further HNO_3.[18,19]

In this work, cellulose nitrate films were prepared and irradiated with a xenon lamp at $\lambda \geq 280$ nm as reference material for Raman microscopy. Due to the recurrent use of camphor in the production of cellulose nitrate films, references of this plasticizer and celluloid (formulation of cellulose nitrate and camphor 70/30% by weight) were also produced for comparison purposes. Overall, we show that with these references, it is now possible, by comparison, to study the degradation of nitrocellulose-based heritage using these two complementary techniques, Raman and infrared spectroscopy.

3 | EXPERIMENTAL

3.1 | Materials

For cellulose nitrate and celluloid films preparation, cellulose nitrate membranes (Hybond™ ECL™, GE Healthcare), racemic camphor (Fragon 33069-27, $C_{10}H_{16}O$), HPLC grade methanol ($\geq$99.9%), demountable quartz cells (Lightpath Optical [UK] Ltd.), and NaCl windows (Thermo Spectra-Tech, 25 mm × 4 mm) were used.

3.2 | Preparation of cellulose nitrate and celluloid films

Cellulose nitrate films were obtained from a solution of 1.85% (w/v) in methanol, prepared at room temperature and allowing cellulose nitrate to dissolve through the night (approx. 12 hr). To analyze the polymer by FTIR, films were prepared on NaCl windows. The solution was applied homogeneously with a Pasteur pipette on the surface of the window. Evaporation of the solvent was accelerated using a heater until a transparent film was obtained. For μ-Raman analysis, the flat side of the demountable quartz cells was covered with this solution using a Pasteur pipette. These cells were placed inside a desiccator with silica gel, and the solution was left drying for at least 3 hr. After drying, transparent cellulose nitrate films, with a thickness lower than 1 μm and well adhered to the quartz cells, were obtained. The good adhesion of the films to the quartz overcame the film embrittlement obstacle during aging.

Celluloid films were obtained adding camphor to the solution, in a 70/30 ratio (cellulose nitrate/camphor), in weight. They were prepared following the same methodology used for the cellulose nitrate films.

3.3 | Preparation of camphor references

A 0.1 M solution in ethanol of racemic camphor ($C_{10}H_{16}O$) was applied on NaCl windows for FTIR analysis. Raman spectra of camphor were acquired in solid state.

3.4 | Cinematographic films

A total of 35-mm cinematographic films were obtained from an aluminum can of the National Archive of Motion Pictures (ANIM, Portugal) labeled as belonging to the film "Man Are That Way" (1939, director Arthur Maria Rabenault). When opened, an intense noxious smell was felt. Within the aluminum box, there are several reels of unknown provenance. The archive of the Portuguese national cinematheque was created in 1948, and in 1996, the conservation center, known as ANIM, was built. It is known from the literature that these films were widely used between the 1890s and the 1950s and that the production ceased in 1951 due to cellulose nitrate flammability. Therefore, these films can date from 1948 to 1951 or earlier. Samples were collected from broken parts or parts without information, from the reels S1, R1, R6, and R14. For μ-FTIR analysis, μ-samples were collected using Ted Pella μ-tools and a Leica MZ16 stereo microscope (between 7.1× and 115×), equipped with a Leica ICD digital camera and a Leica KI fiber optic light system 1500 LCD.

3.5 | Accelerated aging

The irradiation of the films was carried out in a CO.FO. ME.GRA accelerated aging apparatus (SolarBox 3000e) equipped with a Xenon-arc light source, an outdoor filter $\lambda \geq 280$ nm, with constant irradiation of 800 W/m^2 and black standard temperature of 50°C. The films were irradiated for a maximum period of 225 hr (total irradiance = 547 MJ/m^2). Measurements were performed before irradiation and after the following irradiation times (hours): 5, 10, 15, 20, 35, 50, 65, 130, 145, 210, and 225.

3.6 | Infrared spectroscopy

Infrared spectra were acquired on a Nicolet Nexus spectrophotometer equipped with a Nicolet Continuμm (15× objective) microscope and a Mercury–Cadmium–Tellurium detector cooled by liquid nitrogen. The spectra of the cellulose nitrate films were obtained in transmission mode between 4000 and 500 cm^{-1}, with a resolution of 8 cm^{-1} and 64 scans. μ-samples were place on a diamond cell, and the spectra were acquired in transmission mode between 4000 and 650 cm^{-1}, with a resolution of 8 cm^{-1} and 128 scans. Spectra are shown here as acquired, without corrections or any further

manipulation, except for the removal of the CO_2 absorption at approximately 2300–2400 cm^{-1}.

3.7 | μ-Raman spectroscopy

The Raman spectra were collected on a Labram 300 Jobin Yvon spectrometer equipped with a He-Ne laser with a power of 17 mW, operating at 632.8 nm. The laser beam was focused with an Olympus 100× lens with a spot size of 2 μm. The laser was used at maximum power (without the use of filters), with a collection time of 15 s performing 20 to 30 scans. Thermally induced decomposition of the samples did not occur with the experimental conditions used; prior to using the laser at the maximum power, a series of spectra in the same point were acquired using neutral density filters, starting with the highest filtering to the lowest (optical densities 2, 1, 0.6, and 0.3). As the power was increased, no spectral changes were observed, which indicated that no thermally induced decomposition was occurring while using Raman spectroscopy.

3.8 | Micro-energy dispersive X-ray fluorescence

X-ray fluorescence of the cinematographic films was acquired on a Bruker ArtTAX Pro spectrometer equipped with a Molybdenum (Mo) ampule, Peltier effect cooled Xflash 3001® semiconductor detector, and a movable arm. The experimental parameters used were voltage of 40 kV, current of 300 μA, acquisition time of 180 s, and helium atmosphere. A glass slide was placed under each sample studied, and a previous analysis identified the following elements: Si, Ca, K, and Fe.

4 | RESULTS AND DISCUSSION

4.1 | Irradiation of cellulose nitrate films (λ ≥ 280 nm) followed by infrared and Raman

During irradiation, infrared spectra showed an overall intensity decrease of cellulose nitrate absorptions, Figure 2 and Table 1. This agrees with the mechanisms proposed that show continuous chain scission and glyosidic ring opening with the parallel formation of volatile products.[12–16] In Table 1, the main infrared absorption bands are described, comparing very well with recent published values.[7]

In a more detailed analysis, already after 50 hr irradiation, we observe a decrease in intensity of the nitrate group vibration bands at 1655, 1282, and 841 cm^{-1} as a result of the homolytic scission of the NO bond; a decrease in intensity of the polysaccharidic structural
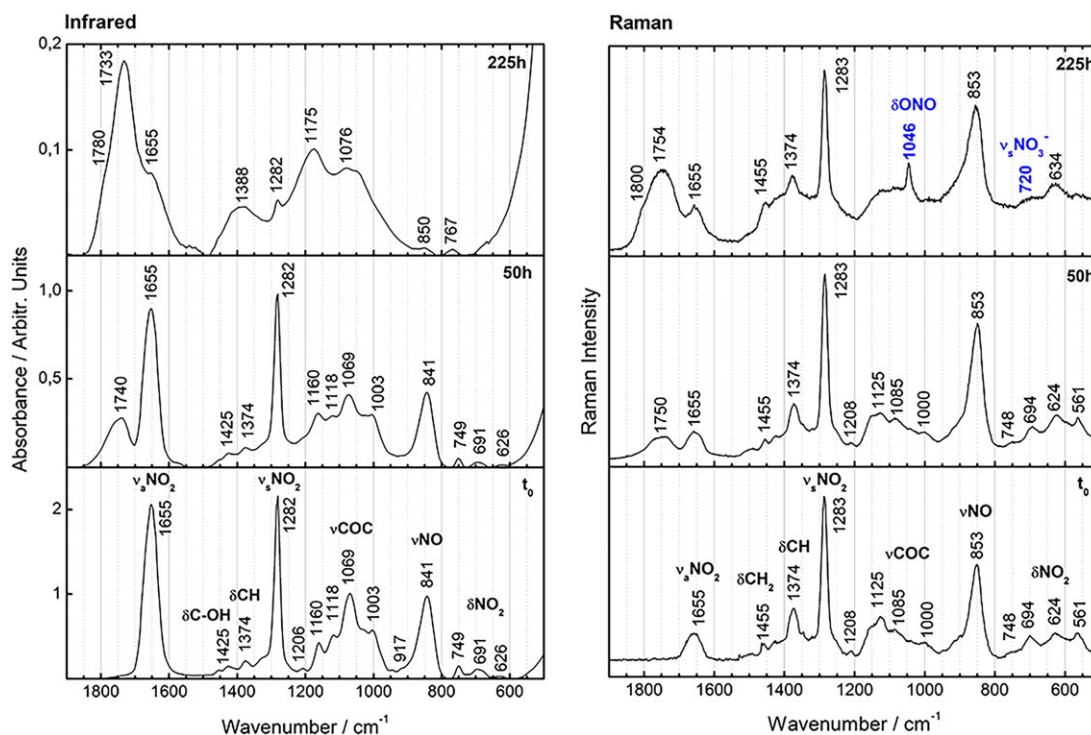

FIGURE 2 Infrared and Raman spectra before (t_0) and after 50 and 225 hr of irradiation of cellulose nitrate films (λ ≥ 280 nm), between 1900 and 500 cm^{-1}. Infrared spectra showed an overall intensity decrease in absorption due to the loss of the nitrate groups, chain scission, ring opening, and volatile emission; and, for $t = 50$ hr, the appearance of a new carbonyl band at 1740 cm^{-1}, which is shifted to 1733 cm^{-1} for $t = 225$ hr. Besides this new carbonyl function, Raman microscopy detected the presence of HNO_3 at 1046 and 720 cm^{-1}

TABLE 1 Main infrared and Raman bands of cellulose nitrate[a,b,c] In bold, the main cellulose nitrate bands [Colour table can be viewed at wileyonlinelibrary.com]

Infrared/cm^{-1}		Assignment	Raman/cm^{-1}			Assignment
This work	literature[7]		This work	literature[9]	literature[20]d	
3570 w	3500 w	νOH[7,16,20–22]				
					3016 s	
2965 w	2965 w	ν_sCH$_2$[21]	**2976 vs**	n/a vs	**2974 vs**	νCH$_2$[e]
2905 w	2905 w	νCH[21]	**2908 s**	n/a s	**2901 s**	νCH[e]
1655 vs	**1650 vs**	ν_aNO$_2$[7,16,20–22]	1655 m	1650 m	1662 m	ν_aNO$_2$[9,20]
1454 w	1460 w	δCH$_2$[7,16,20–22]	1455 w	n/a w	1456 w	δCH$_2$[20]
1425 w		δC—OH[20,22]	1425 w	n/a w	1419 w	δC—OH[20]
1374 w	1375 w	δCH[7,16,20–22]	**1374 s**	**1375 s**	**1366 s**	δCH[20]
1282 vs	**1280 vs**	ν_sNO$_2$[7,16,20–22]	**1283 vs**	**1280 vs**	**1285 vs**	ν_sNO$_2$[9,20]
1206 w		νCOC[7,16,20,22]	1208 w	n/a w		νCOC[20]
1160 m	1160 m	νCOC[7,16,20,22]	1158 sh	n/a m	1156 m	νCOC[20]
1118 m	1120 m	νCOC[7,16,20,22]	1125 m	1120 m	1126 m	νCOC[20]
1069 s	**1060 s**	νCOC[7,16,20,22]	1085 m	n/a m	1087 m	νCOC[20]
1003 m		νCOC[7,16,20,22]	1000 w	n/a w	1001 w	νCOC[20]
917 w	920 w	δring[7,16]			921 w	δCH[20]
841 s	**840 s**	νNO[7,16,20–22]	**853 vs**	n/a vs	**844 s**	νNO[9,20]
749 w	750 w	γ_wNO$_2$[20,22]	748 w	n/a w		γ_wNO$_2$[20]
691 w	690 w	δNO$_2$[7,16,20]	694 m	698 m	696 w	δNO$_2$[20]
626 w		γ_rNO$_2$[20,22]	624 m	n/a m	627 w	γ_rNO$_2$[20]
			561 m	n/a m	561 w	Pyranose[20]

Note. Band assignments are made based on comparison to literature spectra and their assignments; IR, particularly, the work by Bussière et al.[7] and references therein; Raman, the work by Paris and Coupry,[9] using FT-Raman, and Moore et al.[20]

[a]vs: very strong; s: strong; m: medium; w: weak; sh: shoulder.

[b]ν_a: antisymmetric stretching; ν_s: symmetric stretching; δ: scissoring; γ_w: wagging; γ_r: rocking.

[c]n/a, band number not available.

[d]K. Castro et al.[22] used a 514-nm laser.

[e]Due to the more pronounce decrease, during irradiation, of this peak compared with the νCH$_2$ vibration, we assign this vibration to a CH stretching, according to Jutier et al.[21] IR assignment.

bands at 1200–900 cm^{-1} as a result of ring opening and chain scission; the loss of resolution of the νCH at 2965 cm^{-1} and νCH$_2$ at 2915 cm^{-1} due to the more pronounced decrease in intensity of the latter as a result of a preferential hydrogen abstraction at C1, Figure 3; the OH absorption shift to shorter wavelengths together with the appearance of new carbonyl bands, centered at 1740–35 cm^{-1}, reflects the formation of hydroperoxides and carbonyl intermediates. At advanced stages of degradation (225 hr), the broad band attributed to the carbonyl groups is shifted to 1730–1725 cm^{-1} and a shoulder at 1780 cm^{-1} appears, consequence of the transformation of the initial degradation products, Figures 1 and 2.

In Figures 2 and 3, we show the Raman spectra obtained for the irradiated films, 50 and 225 hr, compared with the unaged reference materials. A tentative assignment of the bands, based on the literature, is presented in Table 1. Overall, the results for the main Raman bands in this work (very strong and strong) compare well to the values obtained by Paris and Coupry[9] and reasonably, considering that excitation was performed using a 514-nm laser, with K. Castro et al.[22] In both IR and Raman, the spectra are marked by the intense main vibration bands of the nitrate groups (ONO$_2$).

The first conclusion we draw is that it was not possible to observe the formation of hydroperoxides; no OH bond vibrations were detected in the 4000–3100 cm^{-1} region and for this reason, it is not represented.

On the other hand, the decrease in intensity of the νCH at 2908 cm^{-1}, compared with the νCH$_2$ at 2976 cm^{-1}, is more pronounced and clearly visible already at 50 hr irradiation, which confirms the
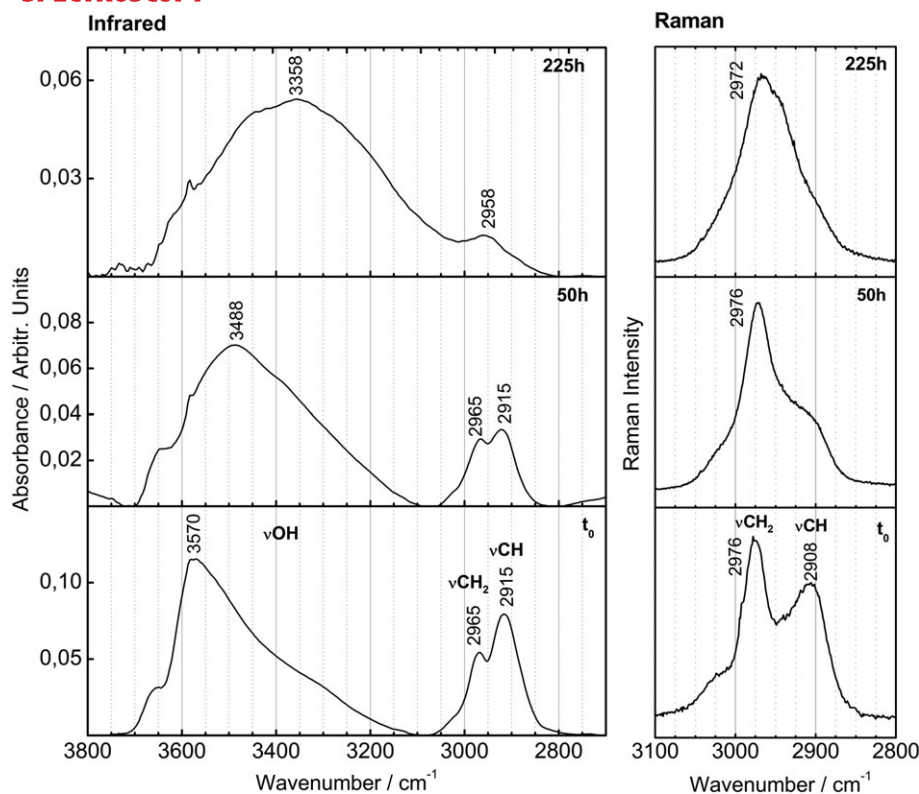
FIGURE 3 Infrared and Raman spectra, 1900–500 cm^{-1} interval, before (t$_0$) and after 50 and 225 hr of irradiation of cellulose nitrate films ($\lambda \geq 280$ nm). The decrease in intensity of the νCH at 2908 cm^{-1}, compared with the νCH$_2$ at 2976 cm^{-1}, is more pronounced and clearly visible already at 50 hr irradiation in the Raman spectra

preferential hydrogen abstraction by the NO$_2$ radical at C1, Figures 1 and 3.[23]

As already observed by infrared spectroscopy, after 50 hr of irradiation, it was possible to identify the formation of a broad band between 1800 and 1700 cm^{-1} characteristic of degradation products with carbonyl functions. Upon 225 hr, this band had a higher relative intensity with a maximum centered at 1754 cm^{-1} and a shoulder at 1800 cm^{-1}, which may be associated with the shoulder observed in the infrared spectra, Figures 1 and 2. This complementarity with infrared spectroscopy reinforces the molecular mechanisms proposed in the literature.

Surprisingly, Raman microscopy identified the presence of nitric acid at advanced stages of degradation (225 hr), Figure 2, by its main peak at 1046 cm^{-1}, Table 2.[24,25] This product was not observed by infrared spectroscopy, possibly due to its low concentration (compared with the polymer matrix). Being a volatile, how can it be detected in the polymer matrix? A possibility is that film polarity and therefore affinity towards water will increase during degradation leading to higher concentrations of nitric acid resulting from the reaction of nitrogen dioxide with water, Figure 1 and Figure S1. Furthermore, degradation leads to a decrease in the degree of substitution, which induces an increase in the diffusion coefficient and permeability of the film.[26] Water molecules can

TABLE 2 Main Raman bands of nitric acid [Colour table can be viewed at wileyonlinelibrary.com]

Raman band/cm^{-1}	Band assignment[a]
1673	ν_aNO$_2$
1430	ν_aNO$_3^-$
1304	ν_aNO$_2$
1046	ν_sNO$_3^-$
955	ν_sN—(OH)
720	δO—N—O
688	δO—N—O$_{(scissors)}$
640	δO—N—O$_{(rock)}$

Note. Band assignments are made based on comparison to literature[24,25].
[a]ν_a: antisymmetric stretching; ν_s: symmetric stretching; δ: deformation.

penetrate more easily into the polymer matrix and the acid formed is entrapped in this polar polymer matrix. In the future, it will be necessary to design an experiment in which the relationship between moisture and the appearance of the nitric acid peak in the Raman is evaluated.

Thus, it becomes only possible to detect HNO$_3$ at high irradiation times. The acid will continue to be produced until nitrate groups (ONO$_2$) are available, as observed in the Raman spectrum at 225 hr, Figure 2. Cellulose nitrate peaks overlap the remaining characteristic peaks of nitric

acid, being only detected a very weak peak at 720 cm^{-1} attributed to the nitrate ion (NO$_3^-$), Table 2.

5 | CASE STUDY: CINEMATOGRAPHIC FILMS

Figures 4 and 5 depict the infrared and Raman spectra for S1, R1, R6, and R14 cinematographic films, naturally aged; these are compared with camphor, unaged cellulose nitrate, and celluloid references. The main changes observed are summarized in Table 3. In the infrared spectra, new carbonyl bands are observed displaying different maxima within the interval 1718–1728 cm^{-1}; the νCH and νCH$_2$ stretching display a different fingerprint and the OH stretching band, usually, is broader for the cinematographic films. This broadening and the appearance of new carbonyl functions agrees with the aging of the cellulose nitrate films, Figures 2 and 3. On the Raman spectra, the new carbonyl functions are also clearly observed. On the other hand, in both infrared and Raman spectra, the C—H fingerprint matches well with celluloid, being indicative of the presence of camphor, which was unequivocally identified by Raman microscopy by its main peak at 650 cm^{-1}, Figure 5. As can be observed in Figures 4 and 5, the carbonyl band of camphor in a cellulose nitrate matrix shifts from 1740/1738 cm^{-1} to lower wavenumbers, 1732/1733 cm^{-1}; this shift is assigned in literature to a hydrogen bonding network.[9,18]
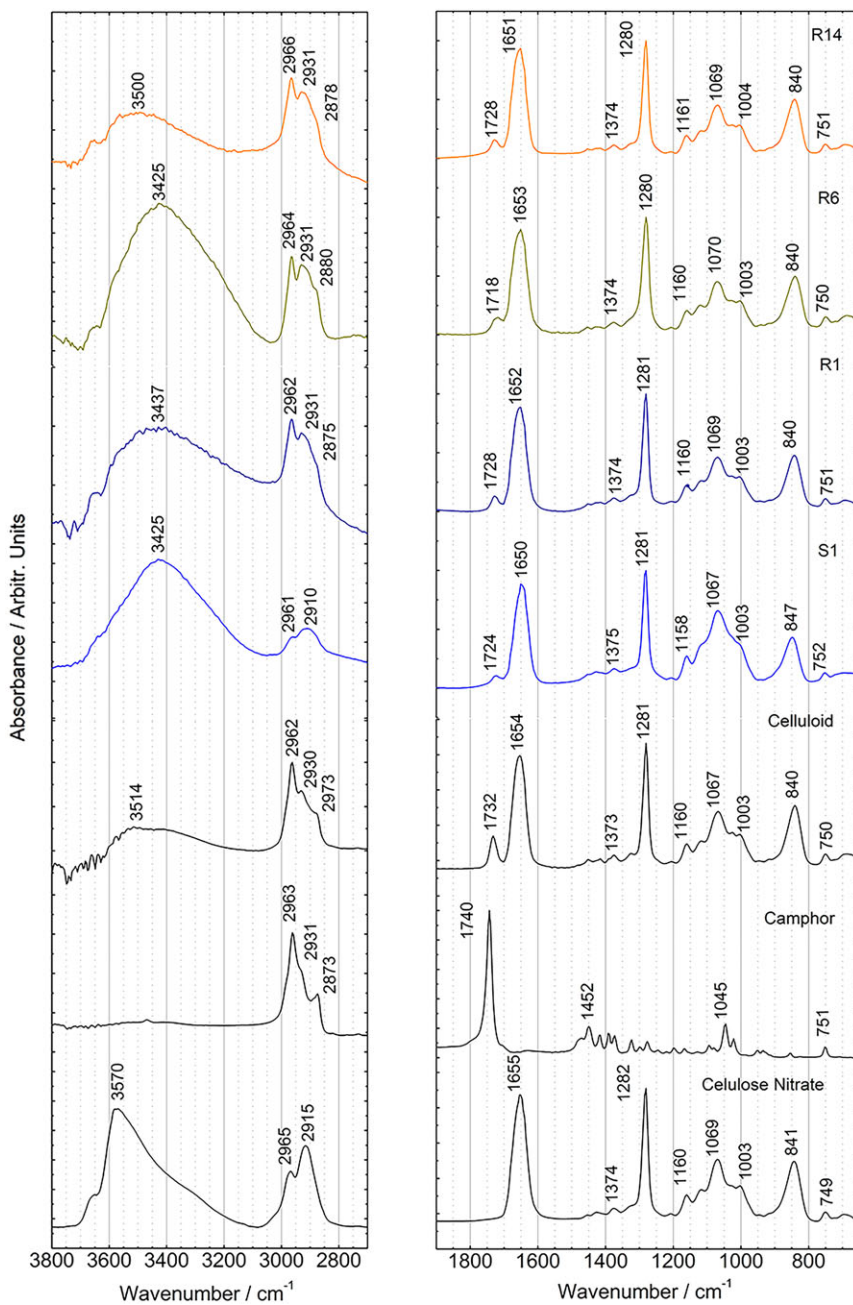

FIGURE 4 Infrared spectra of cellulose nitrate, camphor, celluloid, and of the cinematographic film samples S1, R1, R6, and R14, in the spectral regions 3800–2700 cm^{-1} and 1900–650 cm^{-1}

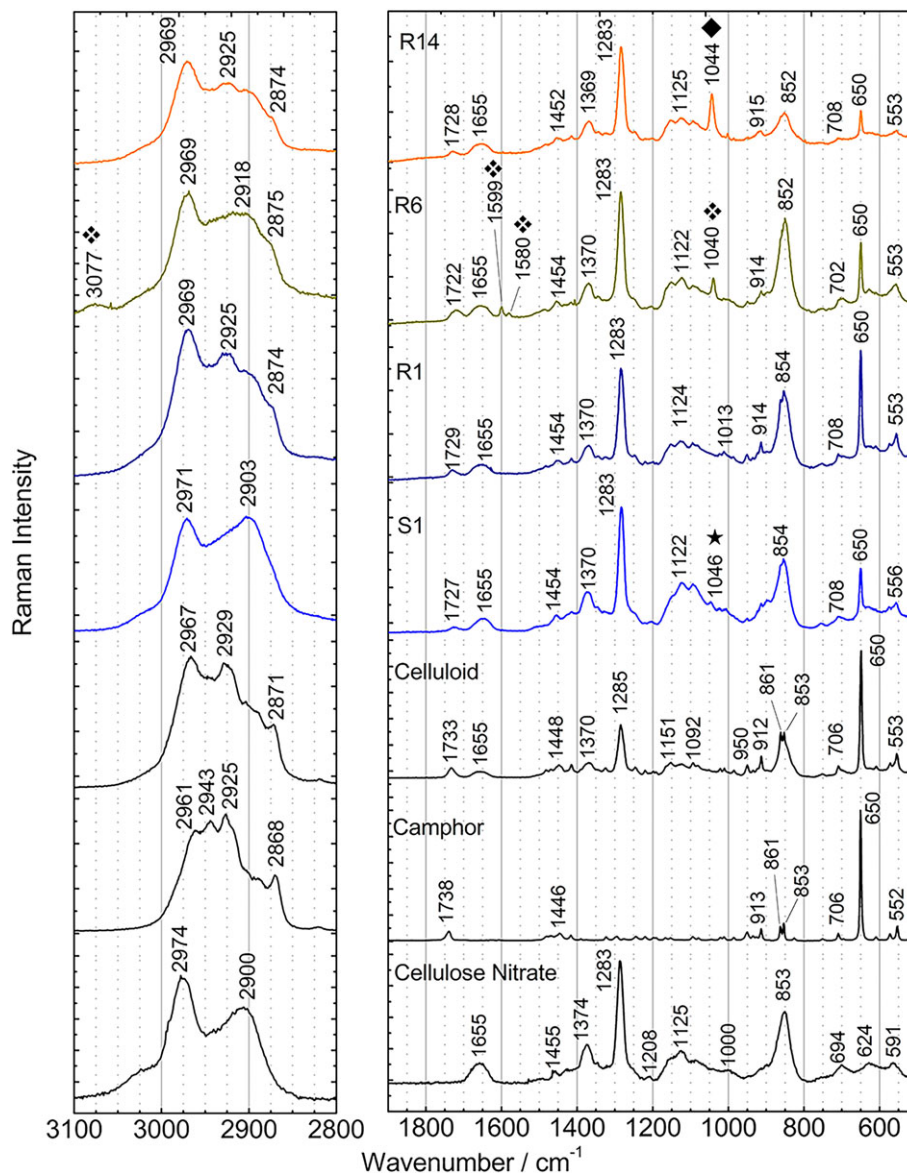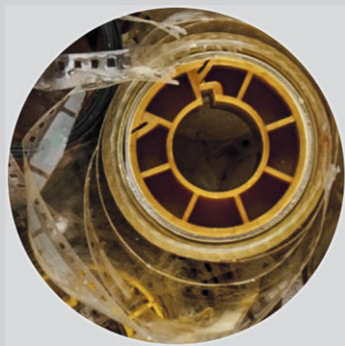**FIGURE 5** Raman spectra of cellulose nitrate, camphor, celluloid, and of the cinematographic film samples S1, R1, R6, and R14, in the spectral regions 3100–2800 cm^{-1} and 1800–500 cm^{-1}. Degradation peaks associated to HNO$_3$ (★), AgNO$_3$ (◆) and to a phthalate plasticizer (❖) were found in samples S1, R14, and R6, respectively

Sample R6 differentiates from the others by the presence of a second plasticizer, identified by Raman microscopy through peaks at 3077, 1599, 1580, and 1040 cm^{-1} assigned to a phthalate, Figure 5.[9,27,28] This plasticizer was not detected in the infrared but it can be the cause for the greater shift of the carbonyl band in the R6 infrared spectrum, Figure 4 and Figure S2. The identification of this plasticizer in this film alone may be associated with its later manufacture date. The most commonly used were diethyl, dibutyl, or dioctyl phthalates but due to their spectral similarities, it was not possible to discriminate which one is present in the film.[4,9] In the future, phthalate references will be produced to allow the full characterization of the plasticizer.

S1 also differentiates from the others in the CH region fingerprint, in which the camphor fingerprint is less visible, indicating a low amount of this plasticizer. In the future, it will be important to quantify the plasticizers in all cinematographic films by Py-GC–MS or/and HR-MS.

Again, Raman microscopy could detect the important degradation products based on HNO$_3$; in sample S1, HNO$_3$ was detected through 1046 cm^{-1} peak, and in R14, silver nitrate (AgNO$_3$) at 1044 cm^{-1}, Figure 5.[24,25,29] This presence of Ag was supported by micro-energy dispersive X-ray fluorescence analysis that did not detect elements in sample S1 but identified silver (Ag) in sample R14, which is respectively related to the lack and presence of a silver image (in cellulose nitrate-

TABLE 3 Reels where the cellulose nitrate-based 35-mm cinematographic film samples were taken from and description of their conservation state

	S1 (1890–1920)[a]	R1 (1890–1920)[a]	R6 (1920–1951)[a]	R14 (1890–1920)[a]
	Sample transparent and without emulsion.	Sample with a yellowed and tacky gelatin emulsion.	Sample with gelatin emulsion but without a silver image.	Sample with a gelatin emulsion and silver image.
	Visually in a good conservation state but brittle on touch.	The silver image is lost. The nitrocellulose base is slightly yellow.	The nitrocellulose base is slightly yellow. The film is tacky.	The nitrocellulose base is transparent. The film is very tacky and the image is being lost.
	No elements detected by μ-EDXRF.	Ag, Br, S	No elements detected by μ-EDXRF.	Ag, S
	Camphor; HNO_3	Camphor	Camphor; phthalate	Camphor; $AgNO_3$
	Carbonyl functions at 1724 cm^{-1} (IR)	Carbonyl functions at 1728 cm^{-1} (IR)	Carbonyl functions at 1718 cm^{-1} (IR)	Carbonyl functions at 1728 cm^{-1} (IR)
	1727 cm^{-1} (Raman)	1729 cm^{-1} (Raman)	1722 cm^{-1} (Raman)	1728 cm^{-1} (Raman)

IR spectra between t_0 and t_{irr} = 50 hr

Note. Elements detected by μ-EDXRF. The degradation products and plasticizers identified by infrared and Raman are listed. A correlation with the irradiated films infrared spectra was made that proposes the degradation stage of the cinematographic films. μ-EDXRF: micro-energy dispersive X-ray fluorescence.

[a]The films provenance is unknown. Film dating is proposed based on the plasticizers identification.

based cinematographic films, the image forming layer was a light-sensitive silver-halide proteinaceous dispersion), Table 3. The detection of these final products further confirms that the artificial aging mechanisms correlate well with the natural aging. The detection of these peaks confirms the noxious environment inside the aluminum can, leading to the reaction of nitric acid with the silver present in the emulsion layer. It should be noted that in R14, the formation of $AgNO_3$ may result from HNO_3 formed in this or other films, for example, film S1.

It is worth noting that in sample R6, the peak at 1040 cm^{-1}, associated with a phthalate, may conceal the nitric acid vibration at 1046 cm^{-1}; an indication that, in the presence of phthalate plasticizers, identification of the HNO_3 using Raman microscopy may be not be possible.

6 | CONCLUSION

For the first time, it was possible to follow the degradation of cellulose nitrate using Raman microscopy. Surprisingly, it was possible to detect in situ the formation of the final product HNO_3, both, in artificially aged samples and in real cases of nitrocellulose cultural heritage (cinematographic films dated from 1890 to 1950). HNO_3 identification shows that S1 cinematographic film is not stable and its presence in the aluminum can is hazardous. Possibly, $AgNO_3$ in sample R14 results from the reaction of HNO_3 formed in S1. On the other hand, the presence of phthalate additives can overlap the nitric acid main peak, being more difficult to evaluate the film condition.

In the artificially aged samples, the presence of HNO_3 is detected in highly degraded cellulose nitrate; it will be necessary to check if this is the case with artworks. Our results were obtained from a small selection of films, and a wider selection will be needed to confirm these very promising results in cultural heritage.

Additionally, compared with infrared spectroscopy, Raman microscopy allowed a straightforward identification of the plasticizers, in particular camphor, used in the cinematographic films. It also allowed the identification of a phthalate plasticizer in one of the samples (R6), possibly due to its later manufacture date. In the future, the molecular characterization of hydroperoxides using Raman spectroscopy will be pursued and the influence of other components in the polymer matrix, namely, camphor in the case of celluloid, will be studied.

ORCID

Artur Neves https://orcid.org/0000-0002-4491-9217
Eva Mariasole Angelin http://orcid.org/0000-0002-9259-674X
Élia Roldão http://orcid.org/0000-0002-6682-7620
Maria João Melo https://orcid.org/0000-0001-7393-6801

REFERENCES

[1] P. C. Painter, M. M. Coleman, *Essentials of Polymer Science and Engineering*, DEStech Publications, Lancaster **2008**.

[2] S. Mossman, *Early Plastics—Perspectives 1850–1950*, Leicester University Press, London **1997**.

[3] R. B. Seymour, G. B. Kauffman, *J. Chem. Educ.* **1992**, *69*, 311.

[4] C. Selwitz, *Cellulose Nitrate in Conservation*, The Getty Conservation Institute, USA **1988**.

[5] M. R. Peres, *The Focal Encyclopedia of Photography*, Taylor & Francis, New York **2007**.

[6] Y. Shashoua, *Conservation of plastics: Materials Science, Degradation and Preservation*, Butterworth Heinemann, Oxford **2008**.

[7] P. O. Bussiere, J. L. Gardette, S. Therias, *Polym. Degrad. Stab.* **2014**, *107*, 246.

[8] N. S. Allen, T. H. Appleyard, M. Edge, D. Francis, C. V. Horie, T. S. Tewitt, *J. Photogr. Sci.* **1988**, *36*, 34.

[9] C. Paris, C. Coupry, *J. Raman Spectrosc.* **2005**, *36*, 77.

[10] O. Madden, K. C. Cobb, A. M. Spencer, *J. Raman Spectrosc.* **2014**, *45*, 1215.

[11] G. Socrates, *Infrared and Raman Characteristic Group Frequencies: Tables and Charts*, 3rd ed., John Wiley & Sons Ltd., Chichester **2001**.

[12] S. Thérias, P. O. Bussière, M. Gardette, J. L. Gardette, A. Lattieu-Derieux, B. Lavédrine, Q. K. Tran, G. Barabant, N. Balcar, A. Colombini, *Actes du colloque Sciences des matériaux du patrimoine culturel* **2012**, *2*, 68.

[13] M. Edge, N. S. Allen, M. Hayes, P. N. K. Riley, C. V. Horie, J. L. Gardette, *Eur. Polym. J.* **1990**, *26*, 623.

[14] M. L. Wolfrom, J. H. Frazer, L. P. Kuhn, E. E. Dickey, S. M. Olin, D. O. Hoffman, R. S. Bower, A. Chaney, E. Carpenter, P. McWain, *J. Am. Chem. Soc.* **1955**, *77*, 6573.

[15] J. Rychlý, A. Lattuati-Derieux, L. Matisová-Rychlá, K. Csomorová, I. Janigová, B. Lavédrine, *J. Therm. Anal. Calorim.* **2012**, *107*, 1267.

[16] S. Berthumeyrie, S. Collin, P. O. Bussière, S. Thérias, *J. Hazard. Mater.* **2014**, *272*, 137.

[17] P. W. Atkins, L. Jones, *Chemistry: Molecules, Matter and Change*, 3rd ed., W H Freeman & Co, New York **1997**.

[18] A. Hamrang, *Degradation and Stabilisation of Cellulose Based Plastics & Artifacts*, Ph.D. thesis, Manchester Metropolitan University **1994**.

[19] S. Babo, E. S. Fragoso, R. J. C. Silva, I. Corte-Real, M. J. Melo, *A Pandoras Box?* , The Aluminum Boxes of Lourdes Castro and the conservation of contemporary art, ICOM-CC Publications **2011**.

[20] D. S. Moore, S. D. McGrane, *J. Mol. Struct.* **2003**, *661-662*, 561.

[21] J. J. Jutier, Y. Harrison, S. Premont, R. E. Prud'homme, *J. Appl. Polym. Sci.* **1987**, *33*, 1359.

[22] K. Castro, S. F. de Vallejuelo, I. Astondoa, F. M. Goñi, J.M. Madariaga, J. Raman Spectrosc. **2011**; 42, 2000

[23] D. Fromageot, N. Pichon, O. Peyron, J. Lemaire, *Polym. Degrad. Stab.* **2006**, *96*, 347.

[24] A. Ruas, P. Pochon, J.-P. Simonin, P. Moisy, *Dalton Trans.* **2010**, *39*, 10148.

[25] N. Minogue, E. Riordan, J. R. Sodeau, *J. Phys. Chem. A* **2003**, *107*, 4436.

[26] M. V. Tsilipotkina, A. A. Tager, L. K. Kolmakova, I. A. Perevalova, V. F. Sopin, G. N. Marchenko, *Polym. Sci. U.S.R. R.* **1989**, *31*, 2201.

[27] T. Nørbygaard, R. W. Berg, *Appl. Spectrosc.* **2004**, *58*, 410.

[28] J. Tsang, O. Madden, M. Coughlin, A. Maiorana, J. Watson, N. C. Little, R. J. Speakman, *Stud. Conserv.* **2009**, *54*, 90.

[29] C.-H. Huang, M. H. Brooker, *Spectrochim. Acta, Part A* **1976**, *32*, 1715.

SUPPORTING INFORMATION

Additional supporting information may be found online in the Supporting Information section at the end of the article.